

# A semi-automatic procedure for digital elevation models generation from stereo digital imagery

Mohamed I. Zahran

Surveying and Photogrammetry Dept., Faculty of Engineering at Shoubra, Benha University, Benha, Egypt

Digital Elevation Models (DEMs) are currently produced by both manual and automated methods. Manual methods are typically reliable, but are slow and expensive for large areas. Automated methods, which determine the ground surface elevation by matching conjugate image portions, can be fast and relatively inexpensive but fail on complicated scenes and in featureless areas. Such automated techniques require the availability of powerful digital photogrammetric workstation with sophisticated software. In this research, a semi-automatic procedure is presented to generate DEMs from stereo digital imagery. Here, the operator points to posts of interest in one image and their conjugate points are found, to sub-pixel accuracy, by use of matching. This would assure selecting appropriate matching entities, leading to a minimal number of matching ambiguities. Moreover, this procedure can be implemented on a PC which is always available in places that can not afford costly photogrammetric workstations. The test imagery consists of a stereo-pair of aerial images covering an urban area. The images are scanned with two different resolutions: 200 dpi and 600 dpi. A total of 90 feature points in the overlapping area are selected and matched using correlation technique. The 3-D ground coordinates of the selected points are computed using bundle adjustment with fixed and inner constraints. Prototype software is developed for matching and adjustment computations. The achieved results have shown simplicity and efficiency of the adopted procedure in reconstructing DEMs from digital aerial imagery.

تنتج النماذج الأرضية الرقمية حالياً بكل من الطرق التي تعتمد على المستخدم بشكل رئيسي والطرق الأوتوماتيكية. النوع الأول يمتاز بالدقة ولكنه بطيء وعالي التكلفة. الطرق الأوتوماتيكية تمكن من تعيين الأرتفاعات الأرضية بعمل توافق أوتوماتيكي للأجزاء المتناظرة من الصور. تمتاز هذه الطرق بالسرعة و التكلفة الأقل ولكنها تفشل في التعامل مع المناطق المعقدة و المناطق الخالية من أية معالم. كما أن هذه الطرق تتطلب وجود أنظمة مسح تصويري رقمية بما تحتوي عليه من برمجيات متطورة. في هذا البحث يتم استعراض اسلوب شبه اوتوماتيكي لتخليق النماذج الأرضية الرقمية من الصور الرقمية المتداخلة. يحدد المستخدم بهذا الاسلوب النقاط المميزة نسبياً على احدي الصورتين و يتم ايجاد النقاط المناظرة في الصورة الأخرى اوتوماتيكياً باستخدام التوافق. ذلك يضمن انتقاء المعالم المناسبة لعملية التوافق مما يحد من المشاكل الناجمة عن عدم وضوح أو تميز هذه المعالم. كذلك يمكن تنفيذ هذا الاسلوب على الحاسوب الشخصي و الذي يتوافر غالباً في معظم الأماكن التي لا تستطيع توفير أنظمة المسح التصويري الرقمية ذات التكلفة العالية. ولغرض اجراء الاختبارات اللازمة اختير زوج من الصور الجوية المتداخلة تغطي منطقة حضرية وممسوحة رقمياً بقدرتي مسح مختلفتين تبلغان مائتي نقطة في البوصة المربعة وستمائة نقطة في البوصة المربعة. تم تحديد تسعون نقطة في منطقة التداخل و أجري لهم التوافق الأوتوماتيكي المبني على الارتباط ثم حساب احداثياتهم الأرضية باستخدام طريقة الحزم الضوئية مع استخدام كلا من الاشتراطات الثابتة و الداخلية و ذلك بواسطة برنامج تجريبي تم تطويره لهذا الغرض. ولقد بينت النتائج المتحصل عليها بساطة الاسلوب المتبنى وكفاءته في تخليق النماذج الأرضية الرقمية من الصور المتداخلة.

**Keywords:** Digital elevation model, Automated photogrammetry, Image matching, Correlation techniques, Digital images

## 1. Introduction

The prevalence of computers has made a significant shift in the way survey and map data are collected, processed, presented and stored. During 1970s, photogrammetric compilers manually traced contour lines from stereo imagery. This contour representation of the terrain, plotted on a stable base material, was the archival medium from which subse-

quent terrain analysis and engineering design were done. Computer capabilities have introduced two fundamental changes to this process. First, terrain data now are collected mostly as a sequence of discrete data (3-D coordinated points). The terrain data, together with other supplementary data, such as abrupt changes in terrain slope or breaklines, set up a discrete sampling of the continuous terrain surface that should be adequate for its

mathematical reconstruction. Second, the archival record has become the digital coordinate file itself rather than a particular graphical depiction, such as contours, profiles, or wire frame perspective views. These depictions can be generated whenever needed as long as the archival data of the original terrain points are available.

DTMs are generally planned such that the collected points lie in a regular grid pattern or represent vertices of local triangular patches in an array referred to as a triangulated irregular network. The advantages of a regular grid layout are a simplified data collection routine, and ease of data access by subsequent programs [5]. The disadvantages are related mostly to the necessity to select a single grid interval, adequate to define the terrain in the roughness area although likely to be over-sampled in regions where the terrain is featureless. Conversely, in the irregular point approach, the sampling interval can change to match the local terrain character. This would optimize the quantity of data necessary to define the terrain. Data access for subsequent software analysis is considerably more involved than when using the simple grid structure.

During the design of a DEM, a quantitative analysis is done to determine the magnitude of the errors expected during reconstruction of the terrain surface. The magnitude of these errors should be within the error budget of potential user or client applications. Given a DEM and interpolation function, one should be able to construct a profile or cross section along any arbitrary path within the area covered. This capability would permit one to interpolate heights at regular grid points from an irregular grid as and to interpolate irregular points from a regular grid. With some cost to accuracy, one could convert between these two popular storage models [6].

Topographic surveys necessary for DEM generation can be performed by photogrammetric methods, terrestrial methods, or some combination of these two procedures. The largest portion of small- and intermediate-scale as well as some large-scale topographic mapping is currently performed by photogrammetric methods. Terrestrial methods are still applicable for large-scale topographic

mapping of small areas and for field completion surveys. However, Global Positioning System (GPS) provides a powerful tool for topographic mapping of extended clear-sky regions.

## 2. Photogrammetric production of DEMs

DTMs are currently produced by both manual and automated methods. In manual production, either the stereoplotters sets the floating mark at the horizontal position of each point and the operator places it on the ground, or the system drives along a profile while the operator keeps the mark on the ground. Automated systems use computer vision techniques to perform the operator's task of determining the ground surface elevation by matching corresponding portions of two stereo images [3,5]. Both production methods have their strengths and weaknesses. Manual methods are typically reliable, but are slow and expensive for large areas. Automated methods can be fast and relatively inexpensive, but fail on complicated scenes, such as urban areas or forests, and in featureless areas. Manual editing of automated results is nearly always required. Some systems let the operator specify complicated areas so that the stereo matcher skips these areas, leaving them for the operator.

The points obtained by image matching are not evenly distributed and do not completely represent the surface. Even if all pixels were selected in image matching, there will be holes since matching is not always successful [7]. Thus the resulted 3-D points must be interpolated. The term surface fitting is more general as it includes interpolation and approximation methods. Surface fitting methods can be classified according to the criteria such as goodness of fit, extent of support (local versus global) or type of mathematical model (weighted average, polynomials, splines).

In most DEM generating systems, matching and surface densification are truly automatic tasks requiring human intervention only in the beginning to initialize the process. Despite all checks performed by the two tasks, it is essential that the DEM is now checked by a human operator for accuracy and complete-

ness, a process that may be referred to as quality control. This interactive process comprises displaying the DEM and editing the data if necessary. The task is very crucial due to its influence on the quality of the DEM and the economy of automated techniques.

### 3. Digital image matching

Image matching, or finding conjugate points automatically, is a fundamental task in photogrammetry. Matching is required in automatic image orientation, automatic aerial triangulation, automatic generation of DEM's and orthoimagery, and object recognition [2,8,10]. The names of matching methods are usually related to the matching primitive, for instance, area-based matching, feature-based matching and symbolic matching.

In area-based matching, gray levels are matched. Here, grey level distribution of small areas of the two overlapping images, named image patches, is compared with each other. The degree of similarity is determined using a maximization criterion such as the cross-correlation coefficient or a minimization criterion as the least-squares technique. In feature-based matching, edges or other features derived from the images are utilized as the matching primitives. Symbolic matching refers to methods that compare symbolic descriptions of images. Symbolic descriptions can be implemented as graphs, trees or semantic nets relating derived image features.

Correlation matching has a well-known procedure for image matching in the field of photogrammetry. The idea is to measure the similarity of the reference window, the image patch that remains fixed in one image, with each of the matching windows in the search window in the other image using the cross-correlation coefficient as follows [6,7]:

$$\rho = \frac{\sum (R_{ij} - \mu_R) (S_{ij} - \mu_S)}{[\sum (R_{ij} - \mu_R)^2]^{1/2} [\sum (S_{ij} - \mu_S)^2]^{1/2}} \quad (1)$$

Where

$R_{ij}$  is the sequence of gray levels contained in the reference window,

$S_{ij}$  is the sequence of gray levels contained in the matching window,

$\mu_R$  is the mean of the sequence of gray levels

contained in the reference window,  $\mu_S$  is the mean of the sequence of gray levels contained in the matching window, and  $\sum \sum$  with  $i$  and  $j$  proceeding over the R-S overlap area.

At performing the matching procedure, the cross correlation coefficient is computed for every position of the matching window within the search window. Next, the position that yields the maximum correlation coefficient is to be determined. If the search window is constrained to the epipolar line, the correlation coefficient can be plotted in a graph and the maximum is found by fitting a polynomial through the correlation values. Otherwise, a two-dimensional polynomial (eq.. 2) is fitted and searched for the maximum.

$$f(x,y) = a_0 + a_1 x + a_2 y + a_3 x y + a_4 x^2 + a_5 y^2. \quad (2)$$

Apart from the used similarity measure, some aspects are crucial and they are to be resolved in order to implement the matching procedure. First, the size and location of the reference window have significant influence on the matching quality. Increasing window size leads to more uniqueness of the matching entity and also to more geometric distortions. Second, the size of the search window affects the duration of processing. Third, the location of the search window is important to provide good approximation for the matching process. Finally, the acceptance and rejection criteria, e.g. threshold values are to be determined carefully after a thorough analysis.

The size and location of the search window are related to the values of  $x$ - and  $y$ -parallaxes. The value of  $y$ -parallax ( $p_y$ ), which differs from one point to another, is a function of the relative orientation between the two images. Such  $y$ -parallaxes can be reduced by bringing the images in epipolar geometry by using their exterior orientation parameters [7]. In epipolar images, lines connecting conjugate points are parallel to the  $x$ -axis of the image coordinate system and have the same  $y$ -coordinate. Accordingly, a point  $(x',y)$  in the right image will be the conjugate of a point  $(x,y)$  in the left image if  $x' = x - p_x$  where  $p_x$  is the  $x$ -parallax of the point. However, since  $p_x$  is un-

known, it can be approximated by the photo base  $b$  of the stereo pair. Thus the point  $(x',y)$  where  $x' = x - b$  serves as the center of the search window. The size of the window in the x-direction is determined by a priori information on the elevation range of the object space. For images taken at height  $H$  above a terrain with maximum elevation range  $\Delta h$ , the maximum parallax range  $\Delta p$  is approximated by the formula  $\Delta p = \Delta h (b/H)$ .

Before starting the correlation process, processing of digital data is usually required to correct for radiometric distortions. Preprocessing usually takes the form of image enhancement such as histogram equalization or linear stretching and filtering using a suitable filter, for example a mean or a median filter [9]. For correlation matching a radiometric adjustment is typically performed prior by equalizing the average and the standard deviation of gray levels of the two conjugate windows, thus accommodating for different radiometric properties of the two images.

The efficiency of correlation techniques can be considerably improved by the use of multi-resolution matching utilizing image pyramid. An image pyramid is formed by successively convolving an image with a gaussian kernel, with each convolution producing a half-resolution copy of the previous image [6,9]. The series of images thus produced can be visualized as a stack of image layers forming a pyramid. By matching images in upper layers of the pyramid, the location of the match can be predicted in lower layers within a couple of pixels, which provides searching through the entire full-resolution image to find a matching feature.

#### 4. The proposed procedure

In this section a semi-automatic approach is proposed to create DEMs from stereo digital imagery. In this procedure, fairly distinct feature points are specified by the operator in one image. By use of correlation matching, the positions of their conjugate points in the other image are found, to sub-pixel accuracy. The 3-D positions of the selected points are computed using least-square solution that is based on collinearity condition equations. The procedure is implemented on a PC using

MATLAB software package. The proposed procedure can be described as follows:

1. Four fairly distinct points that exist in the four corners of the overlap area are identified and measured in the pixel coordinate system of each of the two images. The coordinates of the four pairs are employed in a 2-D transformation to get roughly the conjugate position on the right image for any point specified on the left image.
2. The available control points are identified on the left image. Their coordinates are measured in the pixel coordinate system of the image. They would be used to introduce the datum in the adjustment process.
3. Numerous fairly distinct points on the left image are specified so that the entire image are covered and densified well. Their pixel coordinates are determined and recorded. These points would be the base on which the DEM is generated.
4. For each selected point in the left image, the location of its conjugate is found, to pixel accuracy, in the right image using correlation matching. The reference window is centered at the selected point in the left image whereas the search window is centered at the rough position of its conjugate in the right image.
5. Prototype software is developed to implement the matching process. The program defines the reference window with an appropriate size, enough to define the selected points. The location and the size of the search window are determined using preliminary knowledge about the photography and the terrain. The cross correlation coefficient is computed for every position of the matching window within the search window. The two images must have insignificant differences in scale and orientation; otherwise, they are to be adjusted before.
6. The program looks for the position with the highest correlation value and uses it as the optimal position of the conjugate point, provided that this value exceeds a specified threshold. The location of each conjugate point is found, to sub-pixel accuracy, by fitting a two-dimensional polynomial (with 6-parameters) to the nine pixels centered at the position with the highest correlation, and searching for the maximum. A function is appended to the cross correlation program to deal with this task.

7. For each of the two images, the transformation parameters necessary to convert from the pixel coordinate system, in which the measurements are captured, to the image coordinate systems are computed. This is carried out through the use of calibrated and measured coordinates of image fiducial marks in an affine transformation [5].

8. For each of the two images, convert the coordinates of selected points from the pixel coordinate system to the related image coordinate system.

9. The exterior orientation parameters for each of the two images are found utilizing a space resection procedure based on collinearity condition equations and sufficient ground control.

10. The 3-D coordinates of the collected points are computed using a space intersection process based on collinearity condition equations using the exterior orientation parameters computed formerly in the resection process.

11. The last two steps can be integrated in one simultaneous process (bundle adjustment). This solution provides reliable tools to identify deficient observations and to assess the quality of the whole process.

12. Having higher-resolution copy of the stereo pair, the locations of conjugate points, found in step no. 4, can serve as good approximations for their locations in the higher-resolution images. The coordinates of fiducial marks in both stereo pairs can be employed for the transformation of point coordinates between the corresponding images of the two pairs.

The DEM can be interpolated from the collected points with appropriate grid spacing and interpolation function by using one of available software packages of generating surfaces.

## 5. Experimentation

The test imagery consists of a stereo-pair of aerial photographs, covering an urban area. The scale of photography is nearly 1:2500. The photo pair is scanned with two different resolutions 600 dpi and 200 dpi, yielding nearly 42 $\mu$ m- and 127 $\mu$ m-pixel-size stereo-pairs, respectively [4]. A set of targets are affixed in the photographed area and their 3-D object coordinates are measured using precise terrestrial

surveying to get their coordinates. The two images are shown in figs. 1 and 2, respectively. For each stereo-pair, the coordinates of 4 fairly distinct points in the corners of the overlap area in both images as well as the coordinates of 4 control points and 90 fairly distinct points in the left image are measured using point selection module of MATLAB software. This module enables the user to navigate freely through the image and mark chosen points. The pixel coordinates of marked points are recorded directly by the module. Fig. 3 illustrates the locations of the used control points and the collected DEM points in the overlap area of the stereo pair.

The coordinates of the 4 corner pairs are employed in an affine transformation. The resulted transformation parameters are utilized to get coarsely the conjugate position on the right image for any point selected on the left image. The exact locations of conjugates of the selected points are found automatically, to sub-pixel accuracy, in the right image using the developed cross correlation program. The input data to the program are the pixel coordinates of selected points in the left image and of their coarsely-determined conjugates in the right image. The location of each coarsely-determined conjugate is used as the center of the search window in the right image. For the 200-dpi image pair, the size of the reference window is specified as 7 pixels by 7 pixels, which is enough to describe the selected points in the left image. The size of the search window is taken as 31 pixels by 31 pixels. A matching threshold of 0.6 is selected. The location of each conjugate point is found, to sub-pixel accuracy, by fitting a two-dimensional polynomial to the nine pixels centered at the position with the highest correlation, and searching for the maximum.

For each of the two Images, an affine transformation is employed to convert point coordinates from the pixel coordinate system to the image coordinate system, centered at the principal point. The transformation parameters are computed using the calibrated coordinates of fiducial marks as well as their measured pixel coordinates through a least-squares procedure.

Prototype least-squares bundle adjustment software is developed in order to compute the

exterior orientation parameters for each image and the adjusted object coordinates of collected points. Approximations for the exterior orientation parameters are found using the coordinates of the used control points in both image and object coordinate systems. Enhanced approximate values are obtained from a space resection for each of the two images utilizing ground control points. Approximations for the unknown ground coordinates of the collected points are generated from their coordinates on the left image using parameters of an affine transformation. The transformation is made utilizing ground coordinates of the control points and their left-image coordinates.

Two types of constraints are tried in the adjustment process to introduce absolute information: fixed constraints and inner constraints. Different sets of fixed constraints yield different estimates of the unknown parameters. On the other hand, inner-constraint solution has the minimum magnitude and variance of all possible solutions [1, 5].

The matching results of the 200-dpi stereo pair are used to enhance the efficiency of matching the 600-dpi stereo pair. The coordinates of conjugate points in the 200-dpi right image, obtained by the matching program, are transformed to their equivalent values in the 600-dpi right image. These values serve as good approximations for the centers of the search window in the image. Since the image resolution of the second pair is higher than in the first pair, the size of the reference window is taken larger; 11 pixels by 11 pixels. However, the size of the search window is chosen to be only 21 pixels by 21 pixels due to the refined approximations of conjugate locations.

## 6. Results and analysis

Regarding the used size of the reference and search windows, they were found suitable for detecting almost all conjugate points in the right image. Resulted correlation coefficients, associated with matched points, exceeded 0.8. For the 200-dpi stereo pair, only three conjugate are wrongly detected due to repetitive point pattern within the search window. However, the correct conjugate locations are reached by increasing the size of the reference

window one more pixel in both directions. For the 600-dpi stereo pair, no matching ambiguities have occurred. This is clearly, in addition to the distinctness of selected points, due to adopting search window of limited size considering the related pixel size and size of reference window. This limited size is specified according to the nearly perfect position of the window center provided by the matching results of the 200-dpi stereo pair. Table 1 presents the  $x, y$  image coordinates of selected points in the left image and their conjugates in the right image, found by the matching program.

Table 2 lists standard errors of estimated orientation elements of the left image for four solution setups. Corresponding values for the right image are depicted in table 3. Table 4 gives resulted standard error of unit weight and standard errors of estimated ground-point coordinates in each of the adopted setups. Listed below are the abbreviations used in those tables:

$\sigma_{\omega}, \sigma_{\varphi}, \sigma_{\kappa}$  is the resulted standard errors of estimated orientation angles ( $\omega, \varphi, \kappa$ ),  
 $\sigma_{XL}, \sigma_{YL}, \sigma_{ZL}$  is the resulted standard errors of estimated coordinates of camera perspective center,  
 $\sigma_X, \sigma_Y, \sigma_Z$  is the resulted standard errors of estimated coordinates of ground point, and  
*Ave, Max* average and maximum values.

According to the precision figures listed in the tables 2, 3 and 4, it is clear that the precision gets better at using 600-dpi stereo pair, compared with the 200-dpi stereo pair. Also, the inner-constraint solution has led to better results for both resolutions, compared with the fixed-constraint solution. The resulted standard error of unit weight ( $\sigma_0$ ) in each of the four setups indicates the precision of measured coordinates of matched image points that reached a fraction of a pixel; about one half of a pixel for the 600-dpi stereo pair and nearly one fifth of a pixel for the 200-dpi stereo pair. This denotes the superior precision obtainable by the adopted matching procedure.

Finally, standard errors of computed 3-D ground coordinates of DEM points indicate the good precision resulted utilizing the selected

DEM points, although they normally represent natural features. This is due to the fair distinctness of those points that has led to minimal matching ambiguities and high-quality matching precision.

## 7. Conclusions

In this research, a semi-automatic approach is presented to generate DEMs from stereo digital imagery. In this procedure, the operator points to points of interest in one image and their conjugate points are found, to sub-pixel accuracy, by use of matching. This would enable having suitable matching entities, leading to good matching results. The procedure is implemented on a PC using MATLAB software package. The test imagery

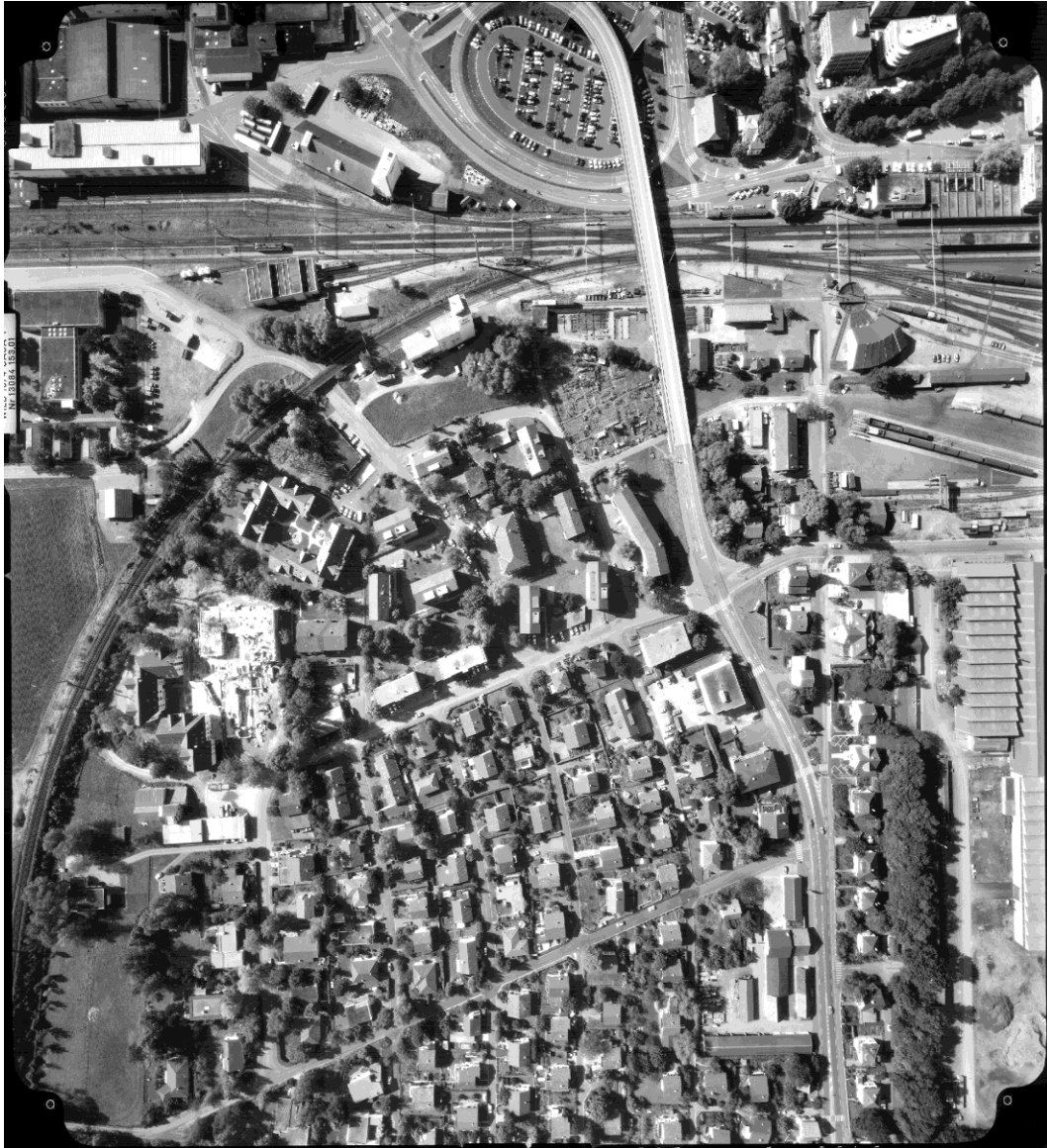


Fig.1. The left image of the test stereo pair.



Fig. 2. The right image of the test stereo pair.

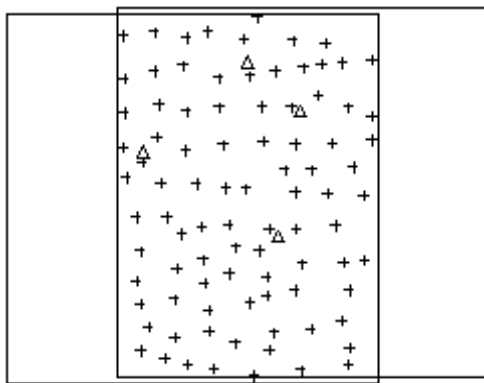


Fig. 3. The configuration of control and DEM points in the overlap area of the stereo pair.

consists of a stereo-pair of aerial photographs, covering an urban area. The scale of photography is nearly 1:2500. The photo pair is scanned with two different resolutions: 600 dpi and 200 dpi. A set of targets is affixed in the photographed area and measured using precise terrestrial surveying. A total of 90 feature points in the overlapping area are selected and matched using correlation technique through prototype software developed in the MATLAB environment. The 3-D positions of the selected points are computed using bundle adjustment with fixed as well as inner constraints. According to the results achieved in this research, a number of conclusions can be drawn as follows:



Table 1  
*x,y* Image coordinates of selected points in the left image and their conjugates in the right image, found by correlation matching

Pt.	Left image		Right image		Pt.	Left image		Right image	
	<i>x</i>	<i>y</i>	<i>X</i>	<i>Y</i>		<i>X</i>	<i>y</i>	<i>x</i>	<i>Y</i>
1	-42.111	101.745	-109.740	97.317	46	106.164	3.081	37.899	-0.533
2	-23.058	103.959	-90.703	99.451	47	89.070	-15.514	20.798	-19.105
3	-3.394	100.458	-70.986	95.911	48	64.684	-17.644	-3.869	-21.408
4	10.084	104.343	-57.377	99.685	49	48.052	-17.835	-20.512	-21.673
5	32.411	99.690	-35.232	94.988	50	22.798	-15.076	-46.129	-18.984
6	40.454	112.860	-26.893	107.800	51	6.288	-16.220	-62.807	-20.214
7	62.485	98.816	-5.430	94.057	52	-15.142	-10.173	-84.707	-14.124
8	82.664	97.154	14.602	92.366	53	-34.315	-10.482	-104.027	-14.522
9	111.185	86.576	42.657	81.961	54	-31.739	-31.308	-101.753	-35.599
10	93.036	85.190	24.712	80.657	55	-9.185	-41.927	-78.956	-46.311
11	80.208	83.968	11.974	79.482	56	-6.174	-20.806	-75.734	-24.914
12	69.104	82.215	0.950	77.804	57	41.901	-30.822	-26.817	-34.791
13	51.611	79.986	-16.325	75.661	58	7.090	-36.403	-62.224	-40.609
14	35.918	76.845	-31.956	72.619	59	22.922	-45.220	-46.336	-49.480
15	16.398	75.478	-51.464	71.274	60	68.146	-39.106	-0.531	-43.026
16	-5.407	83.175	-73.331	78.990	61	63.505	-55.335	-5.276	-59.527
17	-23.074	80.011	-91.077	75.880	62	46.222	-59.078	-22.707	-63.432
18	-41.798	75.117	-110.030	71.096	63	46.401	-47.275	-22.562	-51.433
19	-41.837	54.223	-110.568	50.335	64	94.051	-38.124	25.676	-41.855
20	-20.105	59.346	-88.527	55.400	65	97.022	-55.524	28.601	-59.494
21	17.236	57.796	-51.075	53.808	66	106.752	-36.903	38.457	-40.604
22	-3.473	55.081	-71.959	51.145	67	92.878	-74.293	24.420	-78.587
23	43.328	58.135	-24.931	54.112	68	73.557	-79.551	4.822	-84.065
24	61.607	57.432	-6.641	53.397	69	-31.880	-63.990	-102.545	-68.936
25	78.118	64.590	9.995	60.410	70	-10.919	-61.022	-81.009	-65.764
26	96.752	57.793	28.394	53.723	71	-34.232	-50.083	-104.698	-54.736
27	111.072	51.775	42.624	47.792	72	35.920	-63.292	-33.253	-67.790
28	111.264	37.466	42.769	33.656	73	10.381	-67.892	-59.320	-72.646
29	86.751	35.273	18.467	31.474	74	7.913	-51.383	-61.660	-55.826
30	64.315	34.778	-4.001	30.990	75	-31.497	-92.803	-102.586	-98.544
31	44.325	36.344	-23.948	32.531	76	-10.259	-84.505	-80.664	-89.806
32	-3.774	30.859	-72.386	27.054	77	-26.863	-78.224	-97.682	-83.474
33	19.344	34.454	-49.013	30.679	78	-16.409	-97.555	-87.190	-103.283
34	-21.770	38.937	-90.382	35.097	79	-2.332	-101.225	-72.747	-106.976
35	-42.111	32.667	-110.988	28.863	80	10.580	-80.649	-59.229	-85.687
36	-40.685	14.009	-110.148	10.155	81	26.798	-88.198	-42.716	-93.299
37	-19.242	10.882	-88.285	7.029	82	50.975	-81.510	-18.120	-86.244
38	2.991	10.377	-65.911	6.550	83	38.417	-108.244	-31.193	-113.844
39	21.132	7.770	-47.319	3.941	84	67.251	-105.052	-1.918	-110.250
40	33.573	7.343	-35.058	3.567	85	47.755	-92.287	-21.578	-97.394
41	63.971	5.143	-4.451	1.444	86	13.678	-104.027	-56.412	-109.715
42	83.772	4.053	15.463	0.395	87	96.976	-101.470	28.421	-106.267
43	57.429	19.002	-10.970	15.269	88	97.783	-90.938	29.314	-95.524
44	99.764	20.494	31.424	16.821	89	27.208	-28.800	-41.789	-32.813
45	73.857	18.814	5.536	15.120	90	-30.717	23.709	-99.706	19.868

Table 2  
Resulted standard errors of estimated orientation elements of the left image in different solution setups

Statistic	Fixed-constraint solution (600-dpi Pair)	Inner-constraint solution (600-dpi Pair)	Fixed-constraint solution (200-dpi Pair)	Inner-constraint solution (200-dpi Pair)
$\sigma_{om}$	1.7748	0.5886	2.4341	0.7800
$\sigma_{phi}$	1.2948	0.5649	2.4341	0.7486
$\sigma_{kap}$	0.3918	0.1128	0.5379	0.1495
$\sigma_{XL}$	0.1570	0.0754	0.2157	0.0998
$\sigma_{YL}$	0.2157	0.0715	0.2958	0.0948
$\sigma_{ZL}$	0.0605	0.0223	0.0829	0.0296

Units:  $\sigma_{om}$ ,  $\sigma_{phi}$ ,  $\sigma_{kap}$  are in minutes; and  $\sigma_{XL}$ ,  $\sigma_{YL}$ ,  $\sigma_{ZL}$  are in meters

Table 3  
Resulted standard errors of estimated orientation elements of the right image in different solution setups

Statistic	Fixed-constraint solution (600-dpi)	Inner-constraint solution (600-dpi Pair)	Fixed-constraint solution (200-dpi Pair)	Inner-constraint solution (200-dpi Pair)
$\sigma_{om}$	1.7171	0.5779	2.3550	0.7686
$\sigma_{phi}$	1.3083	0.5810	1.7974	0.7700
$\sigma_{kap}$	0.3902	0.1189	0.5357	0.1576
$\sigma_{XL}$	0.1613	0.0782	0.2246	0.1036
$\sigma_{YL}$	0.2054	0.0701	0.2816	0.0929
$\sigma_{ZL}$	0.07217	0.0227	0.0990	0.0301

Units:  $\sigma_{om}$ ,  $\sigma_{phi}$ ,  $\sigma_{kap}$  are in minutes; and  $\sigma_{XL}$ ,  $\sigma_{YL}$ ,  $\sigma_{ZL}$  are in meters.

Table 4  
Resulted standard error of unit weight ( $\sigma_0$ ) and standard errors of estimated ground-point coordinates in different solution setups

Statistic	Fixed-constraint solution (600-dpi Pair)	Inner-constraint solution (600-dpi Pair)	Fixed-constraint solution (200-dpi Pair)	Inner-constraint solution (200-dpi Pair)
$\sigma_0$	19.4000	17.3000	26.6000	23.0000
Ave $\sigma_x$	0.0826	0.0618	0.1134	0.0820
Max $\sigma_x$	0.1484	0.1121	0.2035	0.1488
Ave $\sigma_y$	0.0687	0.0493	0.0944	0.0653
Max $\sigma_y$	0.1298	0.0970	0.1783	0.1288
Ave $\sigma_z$	0.1947	0.1384	0.2671	0.1835
Max $\sigma_z$	0.2259	0.1412	0.3097	0.1881

Units:  $\sigma_0$  is in  $\mu m$ ; and Ave  $\sigma_x$ , Max  $\sigma_x$ , Ave  $\sigma_y$ , Max  $\sigma_y$ , Ave  $\sigma_z$ , Max  $\sigma_z$  are in meters.

- Due to the power of modern PC platforms, automating DEM generation and other digital photogrammetric procedures can be implemented on PCs.
- The use of multi-resolution correlation matching employing multi-resolution imagery leads to finer approximations, smaller search-window sizes and thus to lesser matching cost and ambiguities.
- Utilizing smaller image pixel sizes enhance the precision of the matching results and the overall adjustment results as well. However, more powerful hardware and software will be required.
- An optimal value of image pixel size is to be found in order to reach the desired DEM accuracy with minimum cost.
- The use of inner-constraint solution is recommended for obtaining improved precision figures.
- To fully automate the entire DEM generation procedure, the presented approach needs one further step; the left-image points are to be derived automatically using feature extraction techniques.

## References

- [1] B. Schaffrin, Advanced Adjustment Computations, Class Notes, Geodetic Science Dept., The Ohio State University, Columbus, OH. (1994).
- [2] C. Heipke, ISPRS Journal of Photogrammetry and Remote Sensing, Vol. 52 (1) 1 (1997).
- [3] C. Heipke, Photogrammetric Engineering and Remote Sensing, Vol. 61 (1), p. 49 (1995).
- [4] DVP Geomatic Systems, DVP Software., DVP Geomatic Systems Inc. (1997).
- [5] E.M. Mikail, J.S. Bethel and J.C. McGlone, Introduction to Modern Photogrammetry, John Wiley and Sons, Inc., New York (2001).
- [6] P.R. Wolf and B.A.Dewitt, Elements of Photogrammetry, McGraw Hill, Inc., New York (2000).
- [7] T. Schenk, Digital Photogrammetry, Laurelville, OH: TerraScience (1999).
- [8] T. Schenk, J.C. Li and C. Toth, Photogrammetric Engineering and Remote Sensing, Vol. 57 (8), p. 1057 (1991).
- [9] W. K. Pratt, Digital Image Processing, John Wiley and Sons, Inc., New York (1991).
- [10] Y. Lue, International Archives of Photogrammetry and Remote Sensing, Vienna, Austria, Vol. XXXI, p. 476 (1996).

Received April 12, 2005  
Accepted October 29, 2005